QUANTIFICATION OF CARDIAC LONGITUDINAL RELAXATION (T_1) AT 3.0 T DURING NORMAL AND HYPEROXIC BREATHING CONDITIONS

By

Paul James Hilt

Thesis

Submitted to the Faculty of the

Graduate School of Vanderbilt University

in partial fulfillment of the requirements

for the degree of

MASTER OF SCIENCE

in

Biomedical Engineering

August, 2008

Nashville, Tennessee

Approved:

Professor Cynthia B. Paschal

Professor James C. Gatenby

ACKNOWLEDGEMENTS

I am indebted to a great number of people who have contributed in many ways to make this work possible. First and foremost on that list is my advisor, Dr. Cynthia Paschal. I arrived at Vanderbilt less than two years ago knowing virtually nothing about MRI or cardiac physiology. Dr. Paschal showed unlimited patience during the many consulting sessions in which she had to explain concepts both simple and difficult to me. Her enthusiasm for the project and her diligent efforts in editing my writings were essential in driving this work to completion. I am also extremely grateful for the assistance of Dr. Brian Welch, who was able to answer an endless string of Philips technology related questions. It would not have been possible to successfully implement and execute the MOLLI code without his help. I would also like to thank Drs. Jeff Luci and Wellington Pham for their consultation and advice in creating the gel phantoms for the sequence validation. Thanks also go to Dr. Chris Gatenby for his efforts in reviewing this paper and offering suggestions for improvement.

Many of my fellow students also contributed to the success of this work. Jared Cobb was helpful throughout the entire project, from teaching me the basics about operating the MRI scanner for cardiac imaging to providing me an example of a well-written thesis. Saikat Sengupta took the initial steps to integrate the MOLLI sequence into the Philips pulse programming environment and provided much continued assistance by showing me the basics of that environment and also helping to debug the code that I added. Jay Moore and Michael Nichols graciously shared their Matlab code for T_1 calculations and

also provided general consulting on various issues for the project. Many other students volunteered their time as research subjects for this study and I am grateful for their participation as well.

I would also like to thank Anna Ambrose and the staff of the Respiratory Care Department for their help in acquiring and storing the breathing gas tanks needed for this study. Robin Avison and Donna Butler were very helpful with patient preparation and the occasional MR software application crisis. Robin also provided a weekly dose of humor with her (mostly) exaggerated imitation of our deep-voiced "breathe in…breathe out" incantation.

Most importantly, I couldn't have done any of this without the love and support of my family. My parents instilled in me a strong work ethic and desire for achievement that was a big factor in my decision to go back to school for a graduate degree. My energetic and entertaining children, Sidera and Parker, provided daily inspiration and laughter that kept me going. Finally, the greatest thank you goes to my loving and supportive wife Analissa, who offered encouragement and assistance in so many different ways. Words cannot express the appreciation that I have for her.

This work was supported by Drs. Cynthia Paschal and John Gore with funding provided by the Vanderbilt University Department of Biomedical Engineering and Vanderbilt University Institute of Imaging Science.

TABLE OF CONTENTS

LIST OF FIGURES

LIST OF TABLES

CHAPTER I

INTRODUCTION

Background

Coronary heart disease is estimated to cause 1 out of every 5 deaths in the United States (1). Over 1.2 million Americans will experience a new or recurring coronary attack in 2008 with a mortality rate near 38%. Early detection of the presence and the extent of a myocardial infarction (MI) is essential for extending the life expectancy of a patient with heart disease.

MRI offers a safe, repeatable method of examining cardiac structure and functionality due to the lack of ionizing radiation used in other cardiac imaging techniques. MRI uses a static magnetic field to align the net magnetic moment from nuclear spins within an imaging sample. These spins then precess about the direction of the static field with a frequency that is proportional to the field strength. The application of a radiofrequency (RF) pulse at the precessional frequency will excite the spins and cause them to rotate into the plane transverse to the static field. Magnetic field gradients are used to select specific locations within the sample to excite and the resulting RF signal produced by the precessing spins is recorded and mathematically transformed to create an image (2).

Contrast in MR images is created through differences in the characteristic magnetization relaxation properties of the tissues or materials contained in a sample, in addition to the

density of the detected spins. These relaxation properties can be quantified as time constants used to represent the exponential longitudinal magnetization recovery (T_1) and transverse relaxation (T_2 & T_2*) times. These time constants are often used to characterize the structural or functional status of living tissues. Increased static field strength leads to longer T_1 values in biological tissue, which contributes to better contrast in cardiac images. This effect, plus the increase in signal to noise ratio (SNR), has driven the increased interest in cardiac imaging at 3.0 T (3).

MRI is a highly effective method of evaluating myocardial ischemia and infarction (4,5). Measurements of T_1 in the heart can be used to determine the relative age and the spatial extent of ischemic myocardial tissue both with and without the use of contrast agents (6). T_1 contrast agents typically consist of paramagnetic particles used to enhance the relaxation rate of the water protons that interact with the agent. Molecular oxygen has been demonstrated as a T_1 contrast agent in the thorax of both humans and small animals at lower field strengths (7,8). The reduction in T_1 during inhalation of pure oxygen in both myocardial tissue and arterial blood of human subjects has been quantified at 1.5 T and 2.0 T (9,10).

T_1 is typically quantified by applying RF pulses that rotate the net magnetic moment either 90°, known as saturation pulses, or 180°, known as inversion pulses, and then sampling the signal intensity at various points during the recovery to equilibrium. Assessment of myocardial T_1 requires a specialized measurement technique to account for the effects of cardiac and respiratory motion. This work selected the Modified Look-

Locker Inversion recovery (MOLLI) technique, which acquires a series of images during three consecutive inversion recovery experiments within a single breath-hold (11). Each image is acquired at a consistent trigger delay from the beginning of the cardiac cycle and each experiment has a unique inversion time relative to the preceding inversion pulse. The MOLLI technique has been demonstrated as repeatable with a characteristic underestimation of less than 10% for reference T_1 values between ~200 and ~1200 ms, corresponding to the expected range of both pre and post-contrast T_1 values for human myocardium and blood at 1.5 T (12).

Objectives and Specific Aims

The primary objective of this research was to quantify the effect of hyperoxia on the longitudinal relaxation (T_1) of myocardium and arterial blood at 3.0 T using a previously demonstrated cardiac T_1 measurement technique known as the MOLLI sequence. An additional objective was to design and evaluate alternatives to the original MOLLI sequence better suited for accurate quantification of the longer T_1 values expected at 3.0 T. The specific aims of this work were the following:

1. To use the MOLLI sequence to measure T_1 in the ventricular septum and left ventricle (LV) blood pool in human subjects during inhalation of compressed medical air and during inhalation of pure oxygen.
2. To evaluate the accuracy and consistency of the MOLLI sequence for reference T_1 values up to 2000 ms, corresponding to the longer expected T_1 values in human myocardium and blood at 3.0 T.

3. To present and evaluate three alternatives to the original MOLLI sequence that are better suited to accurately and consistently quantifying myocardial and blood T_1 at 3.0 T.

Additional Work

Additional work done for this thesis is presented in Chapter 3. This work is not included in the manuscript submitted for publication (Chapter 2) due to its use of assumptions that may not stand up to the peer review process. The purpose of including this chapter is to demonstrate effort taken by the authors to investigate fundamental processes behind experimental results obtained in this study. The accuracy of the findings in this additional work does not affect the validity of the material contained in the manuscript.

In Chapter 3, a theoretical model is presented in order to estimate the expected change in myocardial T_1 with hyperoxia based on the experimental values of normal T_1 in the myocardium and arterial blood in addition to the experimental hyperoxic T_1 of arterial blood. Specifically, a two-compartment, fast-exchange model is used to calculate the theoretical effect of hyperoxia on myocardial T_1.

CHAPTER II

QUANTIFICATION OF CARDIAC LONGITUDINAL RELAXATION AT 3.0 T DURING NORMAL AND HYPEROXIC BREATHING CONDITIONS

Introduction

Recent advancements in high field magnetic resonance imaging (MRI) technology have resulted in increased interest in cardiac imaging at 3.0 T. The higher signal-to-noise ratio (SNR) afforded by increasing field strength offers the potential of enhanced spatial resolution coupled with shortened image acquisition times. Prolonged longitudinal relaxation (T_1) times at 3.0 T can result in increased contrast between normal and infarcted myocardium with the use of T_1-shortening contrast agents (13). However, the increased magnetic susceptibility at higher field strength causes larger static magnetic field (B_0) inhomogeneities, leading to increased susceptibility artifacts that must be addressed through careful selection of image acquisition parameters (14,15).

Quantification of longitudinal relaxation with and without administration of contrast agents is used to characterize a variety of pathological cardiac conditions. T_1 quantification has been shown to be useful as an indicator of tissue perfusion (16,17,18), myocardial infarction (MI) spatial and temporal differentiation (6) and cardiac amyloidosis (19,20). Accurate measurement of tissue T_1 values is also important in the optimization of imaging techniques for high contrast images.

Molecular oxygen is weakly paramagnetic and has demonstrated potential as a contrast agent in MR studies (7,8). Oxygen is inexpensive, readily available, safe in limited durations for healthy subjects and less invasive in comparison to injected contrast agents (21). Typical hemoglobin oxygen saturation levels in healthy humans are greater than 98%. Thus, a large increase in the oxygen content of inhaled air will not lead to a considerable change in the amount of hemoglobin-bound oxygen in the blood, since the hemoglobin is already nearly completely saturated (22). Instead, an elevation of the partial pressure of oxygen (pO_2) in the alveolar space from approximately 100 mm Hg at a normal atmospheric concentration of 21% oxygen to a pO_2 greater than 600 mm Hg at 100% oxygen leads to a similar six-fold increase in concentration of unbound oxygen in the arterial blood (23). Previous studies at 1.5 and 2.0 T have demonstrated up to a 3% reduction in myocardial T_1 and an 11 to 19% reduction in T_1 of arterial blood with exposure to hyperoxia (9,10,24). A 26% reduction in T_1 for in vitro human blood was observed at 1.5 T with increasing oxygen concentration from 21 to 100% (23).

Assessment of myocardial T_1 requires a specialized measurement technique to account for the effects of cardiac and respiratory motion. Since myocardial T_1 at 3.0 T varies by up to 70% during the cardiac cycle (25), it is desirable to assess T_1 by collecting image data at a consistent phase within the cycle. A successful cardiac T_1 measurement sequence must also compensate for respiratory motion during the acquisition of multiple images. This is most commonly done using a patient breath-hold. Collection of image data during a single breath-hold and at a fixed phase of the cardiac cycle eliminates the need for image registration prior to T_1 quantification. Messroghli et al demonstrated an

ECG-triggered, single breath-hold T_1 measurement sequence known as Modified Look-Locker Inversion-recovery (MOLLI) (11). This technique is based on the Look-Locker method of continuous data acquisition following an inversion pulse (26), but was modified to compensate for cardiac and respiratory motion. The MOLLI sequence (Figure 1, as adapted from Messroghli et al, 2004 (11)) consists of images acquired during three sequential inversion recovery (IR) experiments performed during a single breath-hold. The composite image set is reordered (Figure 1) according to the time duration from the corresponding inversion pulse to the data acquisition for each image.

Myocardial T_1 quantification using the MOLLI sequence has been shown to be reproducible at 1.5 T, though the MOLLI sequence characteristically underestimates T_1 by up to 10% compared to reference values between 200 and 1200 ms (11,12). Accurate measurement of T_1 requires complete or near-complete recovery of the longitudinal magnetization between the three IR experiments in a single MOLLI sequence. However, lengthened T_1 at higher field strengths can lead to incomplete magnetization recovery prior to the second and third inversion pulses in the MOLLI sequence, resulting in potential errors in the calculated T_1 values.

The primary objective of this research was to quantify the effect of hyperoxia on the longitudinal relaxation of myocardium and arterial blood at 3.0 T. An additional objective was to design and evaluate alternatives to the original MOLLI sequence better suited for accurate quantification of longer T_1 values at 3.0 T.

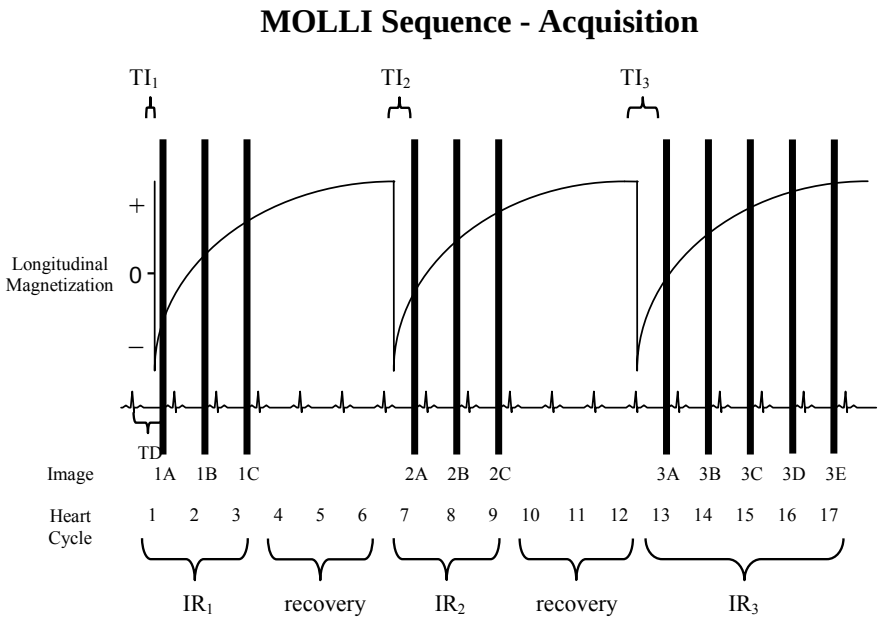

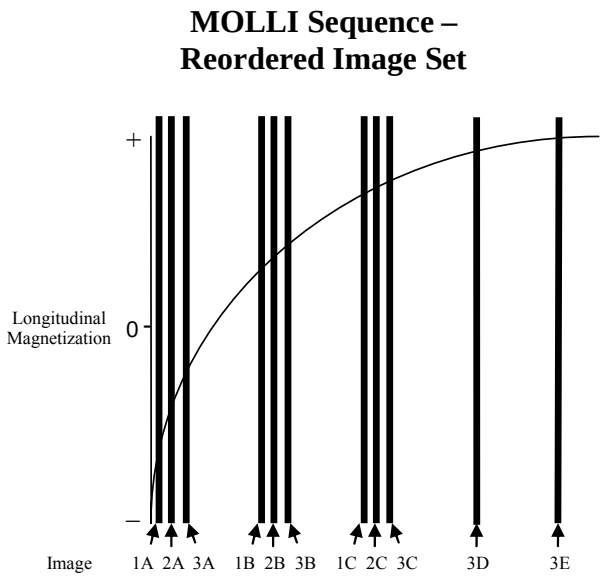

Figure 1. (top) MOLLI sequence diagram, adapted from Figure 1 of Messroghli et al., 2004 (11). Vertical lines represent single-shot images taken at a constant trigger delay (TD) from the R-wave peak. Three successive Look-Locker IR experiments (IR_n) were performed, each with a unique delay from the inversion pulse to the first image acquisition (TI_n). Magnetization recovers undisturbed for three cardiac cycles prior to the second and third inversion pulses in the sequence. The sequence was 17 cardiac cycles in length and performed during a single patient breath-hold. Images were reordered by effective TI prior to curve fitting and estimation of T_1 **(bottom)**.

Materials and Methods

MR studies were performed on a 3.0 T MR system (Intera Achieva, Philips, Best, The Netherlands). Experimental T_1 values were obtained with the MOLLI sequence in healthy volunteers alternately breathing normal air and 100% oxygen. Alternatives to the MOLLI sequence were designed to address the increasing underestimation of T_1 values by the MOLLI sequence at longer reference T_1 values. The MOLLI sequence and the alternatives were validated at different simulated heart rates using phantoms with a range of T_1 values.

In Vivo Oxygen Enhancement Study

Ten healthy volunteers (8 male, 2 female; age = 26.2 ± 3.3 years, range = 22 – 32 years) were recruited to participate in this study. This study was approved by the local institutional review board and informed consent was obtained from all subjects. A six-channel cardiac coil (Philips) was used. Mid-ventricular, short-axis slices were imaged using geometry determined from a real-time scout imaging sequence. Compressed medical air with normal (21%) oxygenation and pure (100%) oxygen were administered at 15 liters per minute alternately using a high-flow oxygen mask with reservoir bag. Images were collected using the MOLLI sequence both before and a minimum of five minutes after switching the subject's breathing source from normal air to pure oxygen.

The MOLLI sequence (Figure 1) consists of three consecutive Look-Locker (26) (LL) IR experiments with three, three and five single-shot images acquired during each respective experiment. Longitudinal magnetization recovers undisturbed for the final three cardiac

cycles of each of the first two LL experiments. Each of the three LL experiments had a different inversion time (TI_n) for the first image in the set. In this work, TI_1 = 100 ms, TI_2 = 300 ms and TI_3 = 500 ms. Subsequent images had an inversion time (TI) determined by summing the TI_n for the current LL experiment with the duration of the preceding cardiac cycles within the experiment. ECG-triggered images were acquired with a constant trigger delay (TD) from the R-wave peak. In order to capture each image during diastole, TD = 550 ms for this study. Each image was acquired with a single-slice, single-shot, balanced steady-state free precession (SSFP or balanced turbo-field echo (bTFE)) readout sequence. Image parameters were: TR/TE/α = 2.3 ms/1.2 ms/30°, acquired pixel size = 1.6 x 2.0 mm, slice thickness = 8 mm, field of view (FOV) = 280 mm x (224 – 252 mm), matrix = 176 x (141 – 159), TFE factor = 70 – 80, with image acquisition duration of 161 – 184 ms. The sequence used a total duration of 17 cardiac cycles and was performed within a single breath-hold.

Image regions selected for analysis included the intraventricular septum and the LV blood pool. T_1 values were computed as described in the following section and a comparison was made between mean T_1 values during inhalation of normal air vs. inhalation of pure oxygen for each selected region.

T_1 Calculations

Images resulting from each T_1 measurement sequence were reordered according to the TI of each image in the set. The durations of the cardiac cycles needed to calculate TI's were extracted from timing information provided in the image header files.

T_1 maps were created for selected regions drawn manually on the image with greatest myocardium to left ventricle (LV) blood pool contrast (MATLAB R2007a; The MathWorks, Natick, MA). Region boundaries were viewed over the image set to verify that image registration was not required.

T_1 values for each pixel within the selected regions were calculated using a three parameter nonlinear curve fitting method, as proposed by Deichmann and Haase (27), for the equation

$$y = A - Be^{\left(\frac{-TI}{T_1^*}\right)}, \quad [1]$$

where y represents signal intensity, A and B are equation coefficients and T_1^* is the apparent T_1 relaxation parameter. Appropriate signal polarity was determined for each time point in the T_1 quantification sequence according to the technique of Nekolla et al (28). This was accomplished by assigning negative polarity to the signal intensity from the shortest TI image in a sequence, executing the fit algorithm and calculating the quality of fit using the correlation coefficient derived from a least squares fit. This procedure was then repeated with negative polarities assigned to the signal intensities for the two shortest TI images, then the three shortest TI images and so on until a maximum fit quality was found via the correlation coefficients.

T_1 values were then calculated from the fit parameters (A, B, T_1^*) for the signal intensity magnitudes (with determined optimal polarities) versus TI from Eq. [1] using

$$T_1 = T_1^*\left(\left(\frac{B}{A}\right)-1\right), \quad [2]$$

which is applicable for T_1 quantification with a Look-Locker technique (27). The mean and standard deviation (SD) of the calculated pixel T_1 values within the selected regions were reported.

Statistics

A paired Student's t-test was used to compare the significance of the change in mean T_1 values for myocardium and LV blood after the volunteers were switched from breathing normal air to pure oxygen. A p-value of < 0.05 was deemed a significant change.

Alternative Pulse Sequences

Three alternatives to the original MOLLI sequence were developed in order to address the error in T_1 quantification for this sequence versus a reference T_1 measurement technique. Each alternative consists of a series of single-shot SSFP images acquired during one or two IR experiments at a consistent trigger delay from the beginning of the cardiac cycle:

1. An alternative 13 cardiac cycle sequence consisting of two consecutive LL experiments (MOLLI Alt. 13-2, Figure 2). Four images are acquired during the

first LL experiment (TI_1 = 100 ms) followed by three cardiac cycles of undisturbed magnetization recovery. Six images are acquired during the second LL experiment (TI_2 = 400 ms). This sequence allows for slightly longer total recovery of the longitudinal magnetization in the first LL experiment, extended sampling time of the magnetization recovery curve and a shortened breath-hold.

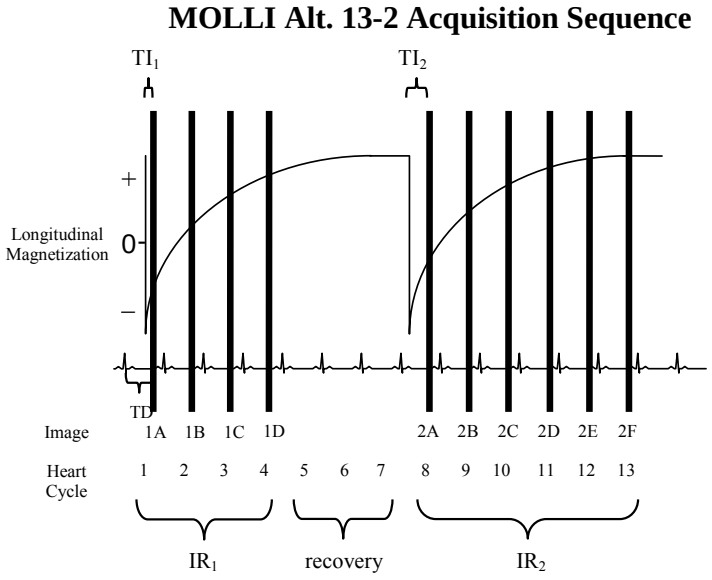

Figure 2. MOLLI Alt. 13-2 sequence diagram. Two successive Look-Locker IR experiments (IR_n) were performed, each with a unique delay from the inversion pulse to the first image acquisition (TI_n). Magnetization recovers undisturbed for three cardiac cycles prior to the second inversion pulse. Images were reordered by effective TI prior to curve fitting and estimation of T_1.

2. A 17 cycle, two LL experiment sequence (MOLLI Alt. 17-2, Figure 3). Six images are acquired during the first LL experiment (TI_1 = 100 ms) followed by six cardiac cycles of undisturbed magnetization recovery. Five images are acquired during the second LL experiment (TI_2 = 400 ms). The longer time delay

between inversion pulses should allow for complete magnetization recovery for T_1 values up to ~1600 ms for heart rates as high as 90 bpm, assuming that a delay of $5*T_1$ is required for full recovery. This sequence also has an extended sampling time that can be useful for longer T_1 samples.

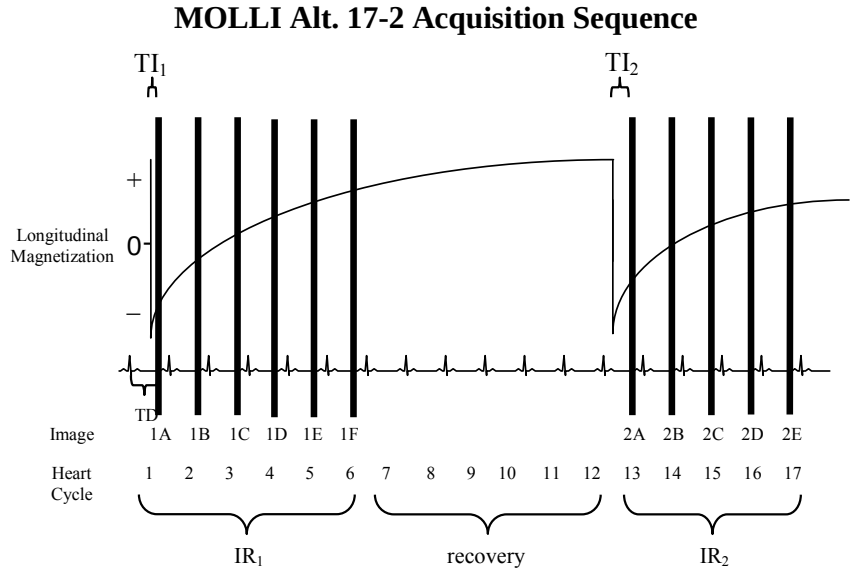

Figure 3. MOLLI Alt. 17-2 sequence diagram. Two successive Look-Locker IR experiments (IR_n) were performed, each with a unique delay from the inversion pulse to the first image acquisition (TI_n). Magnetization recovers undisturbed for six cardiac cycles prior to the second inversion pulse. Images were reordered by effective TI prior to curve fitting and estimation of T_1.

3. A 17 cycle, one LL experiment (TI_1 = 100 ms) sequence (MOLLI Alt. 17-1, Figure 4). This sequence provided a baseline against which to assess the benefit afforded by combining multiple LL experiments into a single sequence. This single inversion sequence takes a single image during each of 17 cardiac cycles. No image reordering is necessary after acquisition.

The images for the MOLLI alternatives were acquired with the same technique and parameters as the images for the original MOLLI sequence.

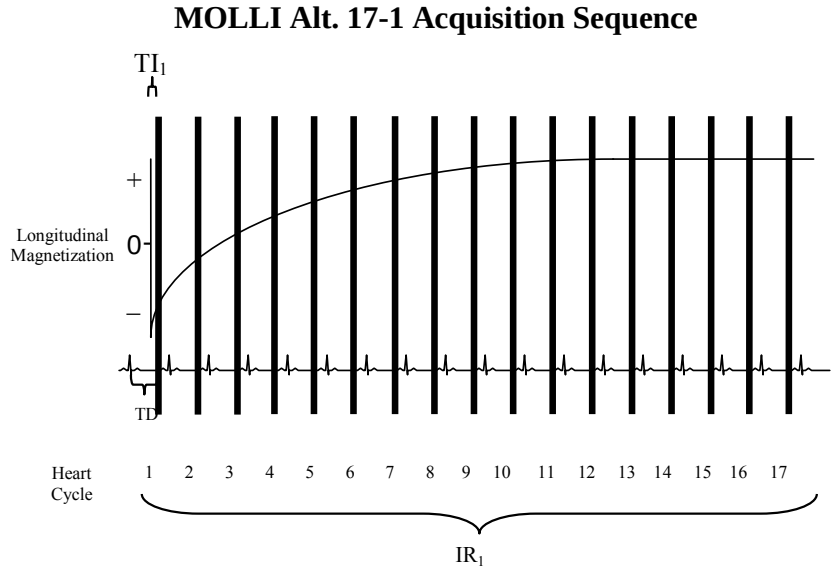

Figure 4. MOLLI Alt. 17-1 sequence diagram. One inversion recovery experiment (IR_1) is performed with one single-shot image acquired during every cardiac cycle. No image reordering is necessary.

Phantom Validation

Nine 2.0% agarose gel phantoms doped with different concentrations of gadoversetamide (OptiMARK, Mallinckrodt Inc., St. Louis, MO) were created in order to assess the accuracy and consistency of T_1 measurements made with the original MOLLI sequence and the three proposed alternatives. All phantom images were obtained with a multi-channel head coil (SENSE-Head 8 coil, Philips). Eight T_1 measurements for each sequence were made at each of three simulated heart rates (40, 60 and 90 beats per

minute (bpm)). The mean T_1 values derived from the eight trials at each simulated heart rate were compared against reference T_1 values. An IR spin-echo technique involving twelve executions with differing TI's was used to find the reference T_1 value for each of the phantoms. The error versus reference T_1 and the coefficient of variance (SD/mean) were reported for each of the four sequences at each reference T_1 value for each simulated heart rate. Phantom image acquisition parameters for the MOLLI and alternative sequences were: TR/TE/α = 2.4 ms/1.2 ms/30°, acquired pixel size = 1.4 x 1.7 mm, slice thickness = 8 mm, FOV = 200 mm x 200 mm, matrix = 176 x 117, TFE factor = 73, with image acquisition duration of 175 ms. Reference IR spin-echo scan parameters were: TR/TE = 12,000 ms/6.4 ms, TI = {50, 100, 200, 300, 500, 750, 1000, 1500, 2000, 3000, 4000, 5000 ms}, acquired pixel size = 2.1 x 3.1 mm, slice thickness = 8 mm, FOV = 200 mm x 200 mm, matrix = 96 x 64, turbo-spin echo (TSE) factor = 4, shot duration = 26 ms.

Results

In Vivo Study

In vivo T_1 values measured with the original MOLLI sequence are shown in Table 1.

Table 1. Experimental T_1 values for selected regions in healthy volunteers (N = 10) breathing compressed medical air (21% oxygen) and pure (100%) oxygen. (* = $p < 0.05$, ** = $p < 0.001$)

	Myocardial T_1 [*ms*]	**LV Blood T_1 [*ms*]**
Normal Air	1175 ± 30	1497 ± 87
Pure Oxygen	1165 ± 35*	1349 ± 104**

There was a small reduction in mean myocardial T_1 in the ventricular septum from 1175 ± 30 ms during breathing of normal air to 1165 ± 35 ms during breathing of pure oxygen

(hyperoxia) ($p < 0.05$, $N = 10$). LV blood T_1 decreased from 1497 ± 87 ms to 1349 ± 104 ms with hyperoxia ($p < 0.001$, $N = 10$). Short axis LV images obtained with the original MOLLI sequence on one subject under normal oxygenation are shown in Figure 5. T_1 maps of the LV myocardium and blood pool during both normal oxygenation and hyperoxia for this subject are shown in Figure 6.

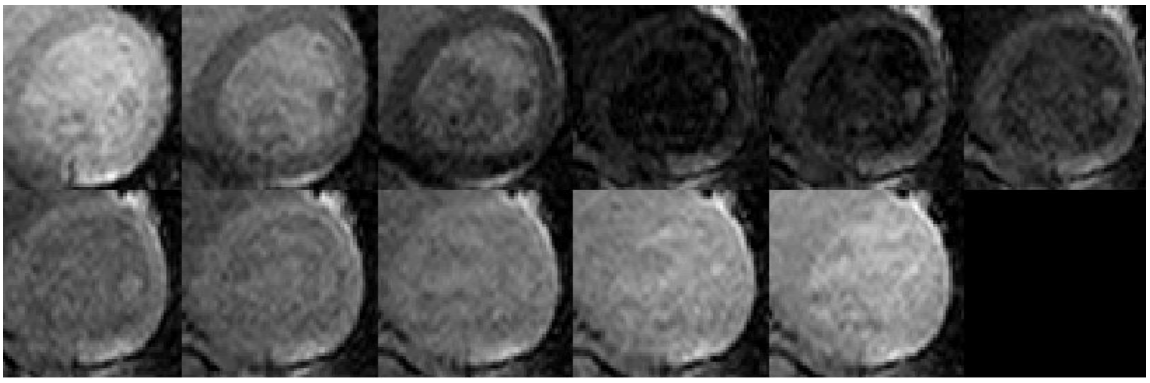

Figure 5. Short axis views of the left ventricle (LV) from images obtained with the original MOLLI sequence on a healthy volunteer. Inversion time (TI) for each image (L to R, top) = 0.10, 0.30, 0.50, 1.10, 1.22, 1.43, (bottom) 2.07, 2.15, 2.39, 3.34, 4.29 sec.

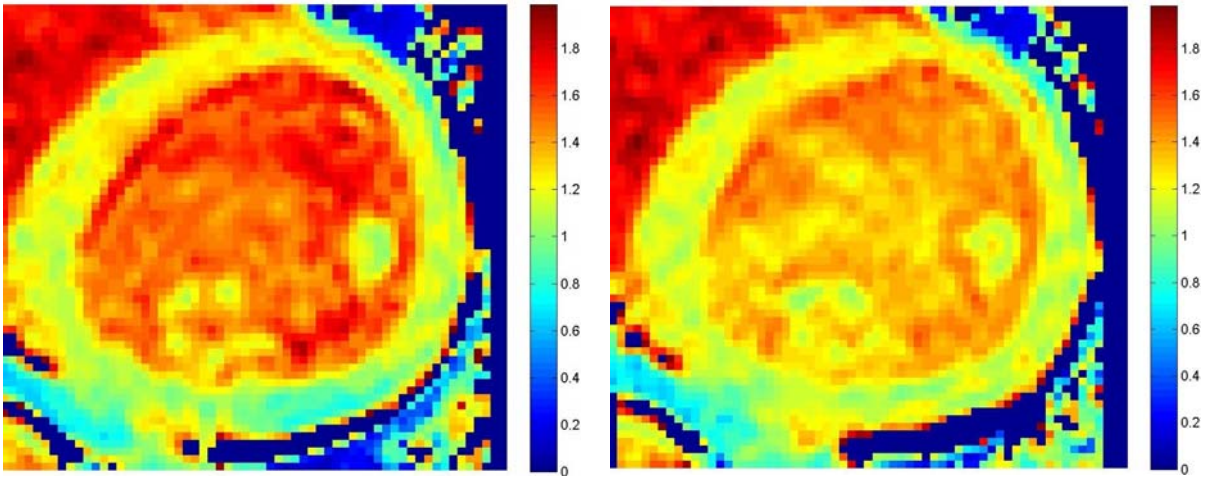

Figure 6. T_1 maps for the short axis view of the LV myocardium and blood pool during normal oxygenation (left) and hyperoxia (right). T_1 values are in seconds. There is an apparent reduction of T_1 values in the LV blood pool while a small but not visually discernable change occured in the myocardium.

Alternative Pulse Sequences and Phantom Validation

The original MOLLI sequence and three proposed alternative sequences (MOLLI Alt. 13-2, MOLLI Alt. 17-2 and MOLLI Alt. 17-1) were evaluated for accuracy and consistency in T_1 measurement by comparison to a reference IR spin-echo technique at three simulated heart rates (40 bpm, 60 bpm and 90 bpm). Mean ± SD T_1 values for all sequences executed on nine gel phantoms with different reference T_1 values at all simulated heart rates are shown in Table 2. The range of reference T_1 values was 420 – 2080 ms.

Table 2. Mean T_1 ± SD calculated from eight iterations of each of the original MOLLI sequence and the three tested alternatives at three simulated heart rates (40 bpm, 60 bpm, 90 bpm).

Sequence	HR	Reference T_1 (ms)								
		420	**574**	**700**	**857**	**1010**	**1226**	**1383**	**1712**	**2080**
Original MOLLI	40 bpm	409 ± 1	553 ± 1	673 ± 1	822 ± 1	959 ± 2	1159 ± 2	1301 ± 3	1604 ± 4	1837 ± 4
	60 bpm	409 ± <1	552 ± 1	669 ± <1	818 ± 1	950 ± 1	1144 ± 1	1275 ± 2	1548 ± 2	1755 ± 1
	90 bpm	408 ± 1	549 ± 1	666 ± 1	807 ± 2	932 ± 1	1099 ± 2	1220 ± 2	1448 ± 2	1607 ± 3
MOLLI Alt. 13-2	40 bpm	409 ± <1	552 ± 1	675 ± 1	821 ± 2	959 ± 2	1161 ± 2	1304 ± 3	1613 ± 4	1861 ± 5
	60 bpm	409 ± <1	551 ± 2	672 ± 1	817 ± 1	953 ± 1	1153 ± 1	1290 ± 3	1582 ± 1	1823 ± 2
	90 bpm	409 ± <1	550 ± 1	671 ± 2	816 ± 2	947 ± 2	1138 ± 3	1266 ± 4	1532 ± 4	1740 ± 4
MOLLI Alt. 17-2	40 bpm	409 ± 1	551 ± 1	674 ± 1	821 ± 1	958 ± 1	1161 ± 1	1305 ± 3	1618 ± 4	1872 ± 4
	60 bpm	408 ± <1	551 ± 1	672 ± 1	818 ± 1	955 ± 1	1158 ± 2	1299 ± 3	1607 ± 2	1872 ± 3
	90 bpm	409 ± <1	550 ± 1	671 ± 2	819 ± 2	955 ± 2	1160 ± 3	1299 ± 3	1610 ± 3	1858 ± 4
MOLLI Alt. 17-1	40 bpm	408 ± 1	545 ± 5	668 ± 3	816 ± 3	953 ± 1	1161 ± 2	1307 ± 3	1623 ± 3	1898 ± 4
	60 bpm	408 ± 2	548 ± 2	667 ± 2	819 ± 1	957 ± 1	1165 ± 2	1310 ± 2	1625 ± 3	1924 ± 3
	90 bpm	409 ± 2	550 ± 2	673 ± 3	825 ± 3	965 ± 4	1178 ± 4	1330 ± 6	1657 ± 5	1943 ± 6

The original MOLLI sequence had the greatest mean and maximum error at each heart rate (Figure 7). In contrast, MOLLI Alt. 17-1 was the most accurate of the four sequences with the smallest mean error at 60 and 90 bpm, mean error within 0.2% of the smallest mean error at 40 bpm and the smallest maximum error at each heart rate. MOLLI Alt. 17-2 and MOLLI Alt. 13-2 generally had the second and third smallest error, respectively. T_1 error increased with reference T_1 values up to 2000 ms for all sequences except MOLLI Alt. 17-1 at each simulated heart rate. In addition, both mean and maximum T_1 error increased with heart rate for all tested sequences except MOLLI Alt. 17-1.

Variance in measured T_1 was very small and consistent across reference T_1 values for the original MOLLI sequence and the two-inversion alternative sequences (MOLLI Alt. 13-2, MOLLI Alt. 17-2) (Figure 8). The mean variance was less than or equal to 0.2% and the maximum variance was less than or equal to 0.4% for these three sequences at each simulated heart rate. MOLLI Alt. 17-1 had the greatest mean and maximum variance for each of the three heart rates with larger error at shorter reference T_1 values. These results indicate that MOLLI Alt. 17-1 is the least consistent of the four tested sequences at reference T_1 values of less than ~1000 ms. However, the coefficient of variance was still less than one percent for this sequence for all reference T_1 values at each heart rate.

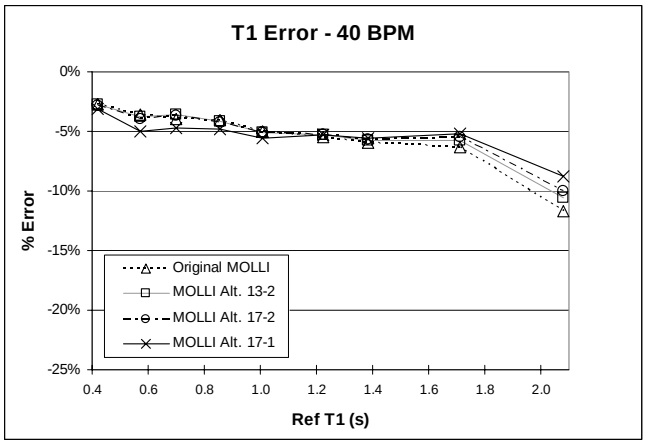

a

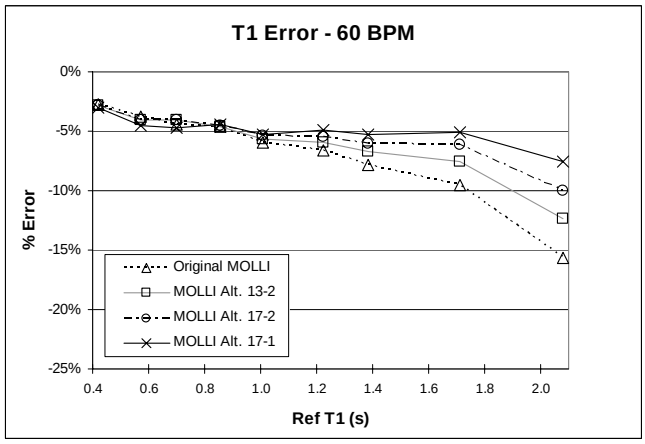

b

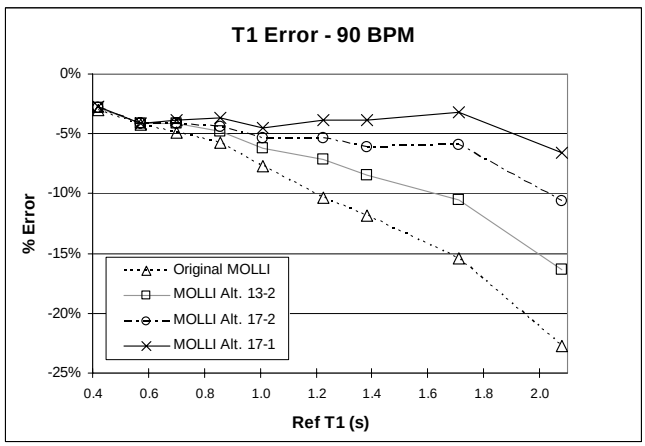

c

Figure 7. Error in mean T_1 values calculated with the original MOLLI sequence and MOLLI Alternatives 13-2, 17-2 and 17-1 vs. reference T_1 for simulated heart rates of (a) 40 bpm, (b) 60 bpm and (c) 90 bpm. The original MOLLI sequence demonstrates the largest error for all three heart rates for reference T_1 values > 1.0 s, while MOLLI Alt. 17-1 shows the least error over the same range. T_1 error generally increases with reference T_1 and heart rate for all four sequences.

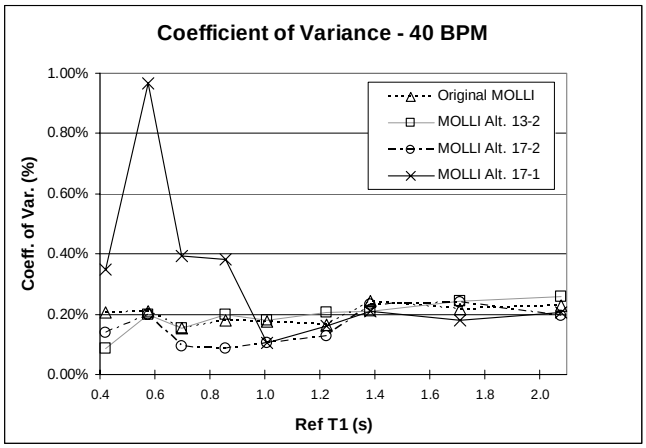

a

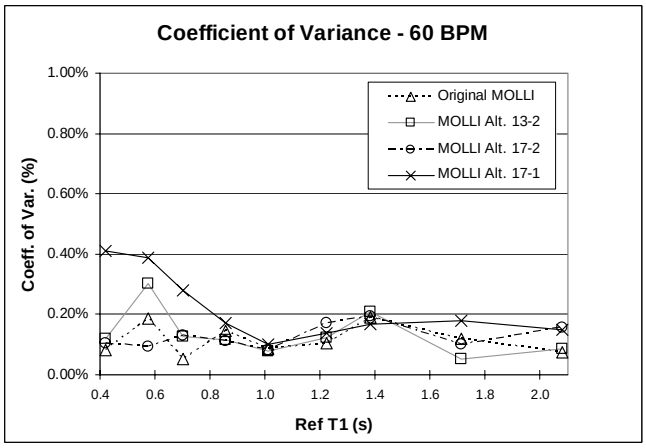

b

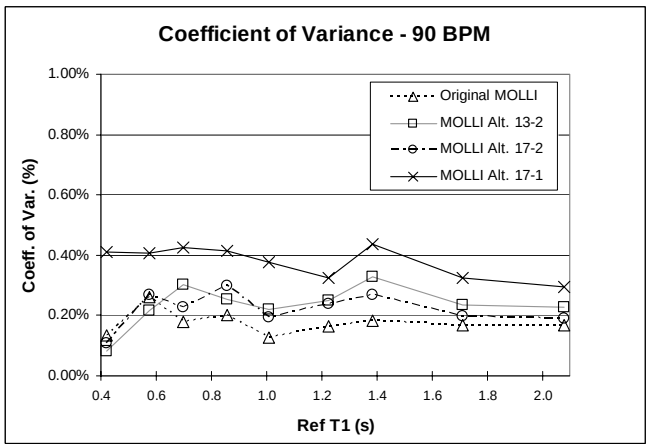

c

Figure 8. Coefficient of variance (SD/mean) for T_1 values calculated with the MOLLI sequence and MOLLI Alternatives 13-2, 17-2 and 17-1 vs. reference T_1 for simulated heart rates of (a) 40 bpm, (b) 60 bpm and (c) 90 bpm. Coefficient of variance is similar for the original MOLLI sequence and MOLLI Alternatives 17-2 & 13-2 over all reference T_1 values and heart rates. MOLLI Alt. 17-1 shows a noticeably higher variance at 90 bpm and for lower reference T_1 values at 40 & 60 bpm.

Discussion

The original MOLLI sequence quantified the mean T_1 value of myocardial tissue in the ventricular septum during normal breathing conditions at 3.0 T as 1175 ± 30 ms. This value is 3.7% lower than published results for mean T_1 of the myocardium (1220 ± 70 ms) in a previous 3.0 T study by Sharma et al (29). Mean LV blood T_1 at 3.0 T was 1497 ± 87 ms in the current study compared to 1660 ± 60 ms in the previous 3.0 T study (29). This represents a 9.8% difference. The MOLLI sequence enables T_1 quantification in a single breath-hold compared to four separate breath-holds required for the previous 3.0 T study (29) and also contains more sample points along the recovery curve (11 vs. 4). In addition, some misregistration occurred in the previous 3.0 T study due to the trigger delay spanning two cardiac cycles (29). This indicates that the images were not acquired at the same phase of the cardiac cycle, which will affect the calculated T_1 due to the variation of myocardial T_1 with cardiac phase (25). This phase difference may account for the relatively large difference in the standard deviations of the myocardial T_1 measurements between the two studies (30 vs. 70 ms, N = 10 for both studies). In addition, the myocardial T_1 value reported by Sharma et al is an average of T_1 values found in the septum and posterior wall. T_1 in the septum was found to be longer than in the posterior wall by 3 – 5% at lower field strengths (12), indicating that the difference in mean calculated septal T_1 between the current study and the previous study may be slightly larger than 3.7%. The underestimation in myocardial and LV blood T_1 for the present study compared to the previous study is consistent with the systematic underestimation for the MOLLI sequence noted by Messroghli et al (11). The amount of underestimation is also similar to the amount demonstrated for similar reference T_1

values in the phantom results of the present study for a heart rate of 60 bpm (average heart rate = 64 bpm for human subjects in this study).

The results of the current study indicate a smaller change in mean myocardial T_1 with hyperoxia at 3.0 T compared to published results at lower field strengths (9,10). Mean T_1 in the myocardial septum was lowered by 0.9% from 1175 ms to 1165 ms in the current study. Mean LV blood T_1 was reduced from 1497 ms to 1349 ms, a difference of 9.9%. Comparable literature results at 1.5 T indicate a 2.9% reduction for T_1 in the myocardium and an 11.3% reduction for arterial blood T_1 with hyperoxia (N = 6) (9). A study at 2.0 T reported a 2.7% decrease in myocardial T_1 and a 16.7% decrease in LV blood T_1 (N = 7) (10).

An evaluation of the relative impact of oxygen as a contrast agent on the myocardium versus arterial blood can be performed by calculating the ratio of the change in relaxation rate of the two regions after administration of the contrast agent ($\Delta R_{1,myo}/ \Delta R_{1,blood}$) (29). The ratio of $\Delta R_{1,myo}/ \Delta R_{1,blood}$ [s^{-1}/s^{-1}] for this study at 3.0 T was 0.10. Values derived from previous studies at 2.0 T and 1.5 T were 0.17 and 0.30, respectively (9,10). The compartmental influence of oxygen as a contrast agent in the myocardium compared to arterial blood appears to be reduced with increasing field strength for these three studies. This comparison is limited by the fact that different T_1 measurement techniques were used between the three studies and the small number of subjects used within each study. However, each study internally used a consistent technique to obtain normal and hyperoxic T_1 values for myocardium and arterial blood. Therefore, the comparison of

changes in T_1 (represented by $\Delta R_{1,myo}/\ \Delta R_{1,blood}$) between myocardium and arterial blood during breathing of pure oxygen within each study should be valid. This allows for a general comparison to be made between studies by observing the $\Delta R_{1,myo}/\ \Delta R_{1,blood}$ ratios. Further studies with a larger number of subjects must be done to definitively report the relative effect of oxygen as a contrast agent at different field strengths.

Underestimation in T_1 quantified with the original MOLLI sequence for T_1 values from 1010 – 1712 ms, corresponding to expected normal myocardial and LV blood T_1 values at 3.0 T, is between 5 – 10% at 40 and 60 bpm in this study. T_1 underestimation in the same range at 90 bpm is between 8 – 15%. The error in T_1 increases with both reference T_1 and heart rate for the original MOLLI sequence (Figure 7). In contrast, the alternative MOLLI sequences were more accurate for these physiologically relevant pre-contrast T_1 values across all heart rates. In the presentation of the original MOLLI sequence, Messroghli et al noted a systematic T_1 underestimation of less than 10% for lower reference T_1 values between 191 – 1196 ms at simulated heart rates from 40 – 100 bpm (11). The present study used extended reference T_1 values of greater than 1200 ms in order to represent the longer in vivo T_1 values expected at 3.0 T. Error in T_1 estimation with the original MOLLI sequence is of greater concern at 3.0 T compared to 1.5 T due to the increasing underestimation that occurs at larger reference T_1 values.

T_1 error was lowest over the pre-contrast T_1 range for myocardium and blood for MOLLI Alt. 17-1 across all three simulated heart rates. This sequence was implemented with a duration of 17 cardiac cycles in this study to be comparable in length to the original

MOLLI sequence. The number of images acquired should be reducible without loss of accuracy or increased variance for MOLLI Alt. 17-1 since longitudinal relaxation should be well-recovered for T_1 values of up to 2000 ms approximately 10 seconds ($5*T_1$) after the inversion pulse. The number of cycles required to achieve this recovery depends on the heart rate. This reduction in length can be used to create shorter breath-hold times.

The coefficient of variance for MOLLI Alt. 17-1 was comparable to the other tested sequences for reference T_1 values greater than 1000 ms at 40 and 60 bpm. Variation was slightly higher for MOLLI Alt. 17-1 in this range at 90 bpm but was still less than 0.5%, indicating good consistency of T_1 estimation. The coefficient of variance for T_1 values of less than 1000 ms at all simulated heart rates was higher for MOLLI Alt. 17-1 compared to the other tested sequences. However, variation was less than 1% across all reference T_1 values (min. 420 ms) for all tested sequences.

The lower limit for myocardial T_1 at 3.0 T with the use of clinically relevant concentrations of gadolinium-based contrast agents is around 400 ms (29). Thus, MOLLI Alt. 17-1 yields a consistent, highly accurate T_1 estimation for the range of pre and post-contrast myocardial T_1 values at 3.0 T. This sequence is equivalent to a triggered Look-Locker acquisition with one image acquired during each cardiac cycle following the inversion pulse. The results of this study indicate that there appears to be little appreciable benefit to the multiple IR-experiment approach of the MOLLI technique for quantifying myocardial T_1 with or without the use of contrast agents at 3.0 T.

The increasing underestimation of T_1 with both reference T_1 and heart rate that is observed with the original MOLLI sequence and MOLLI Alt. 13-2 is attributable to incomplete inversion recovery from the first IR experiment in each sequence. Subsequent recovery curves are sampled at higher than expected signal intensities, leading to a fitted recovery curve with a shortened T_1. This effect is demonstrated in Figure 9 using simulated results with T_1 = 1600 ms and a heart rate of 90 bpm. The increased longitudinal magnetization recovery time for MOLLI Alt. 17-2 (12 cardiac cycles vs. 7/6 cardiac cycles for MOLLI Alt. 13-2/original MOLLI) eliminates this effect for the physiologically relevant range of T_1 values and causes the error for this sequence to remain relatively constant across heart rates.

Messroghli et al attribute the systematic underestimation of T_1 by the MOLLI sequence to the effect of the image acquisition technique on the recovery curve (11). It is noted that image acquisition causes the longitudinal magnetization to recover to an asymptotic value more rapidly than in the case of undisturbed recovery. This early approach to a steady-state value leads to a lower estimated T_1. Though it has been demonstrated that this effect exists for spoiled gradient echo readouts (e.g., Snapshot-FLASH), this phenomena does not appear to occur with SSFP imaging (30). In fact, the reduced impact of the readout technique on the recovery curve was a major factor in the selection of the SSFP technique over spoiled gradient echo for image acquisition in the original MOLLI sequence (11). The source of the systematic underestimation for shorter reference T_1 values, where incomplete recovery prior to later inversion pulses is not a factor, and for the single inversion MOLLI Alt. 17-1 sequence requires further study.

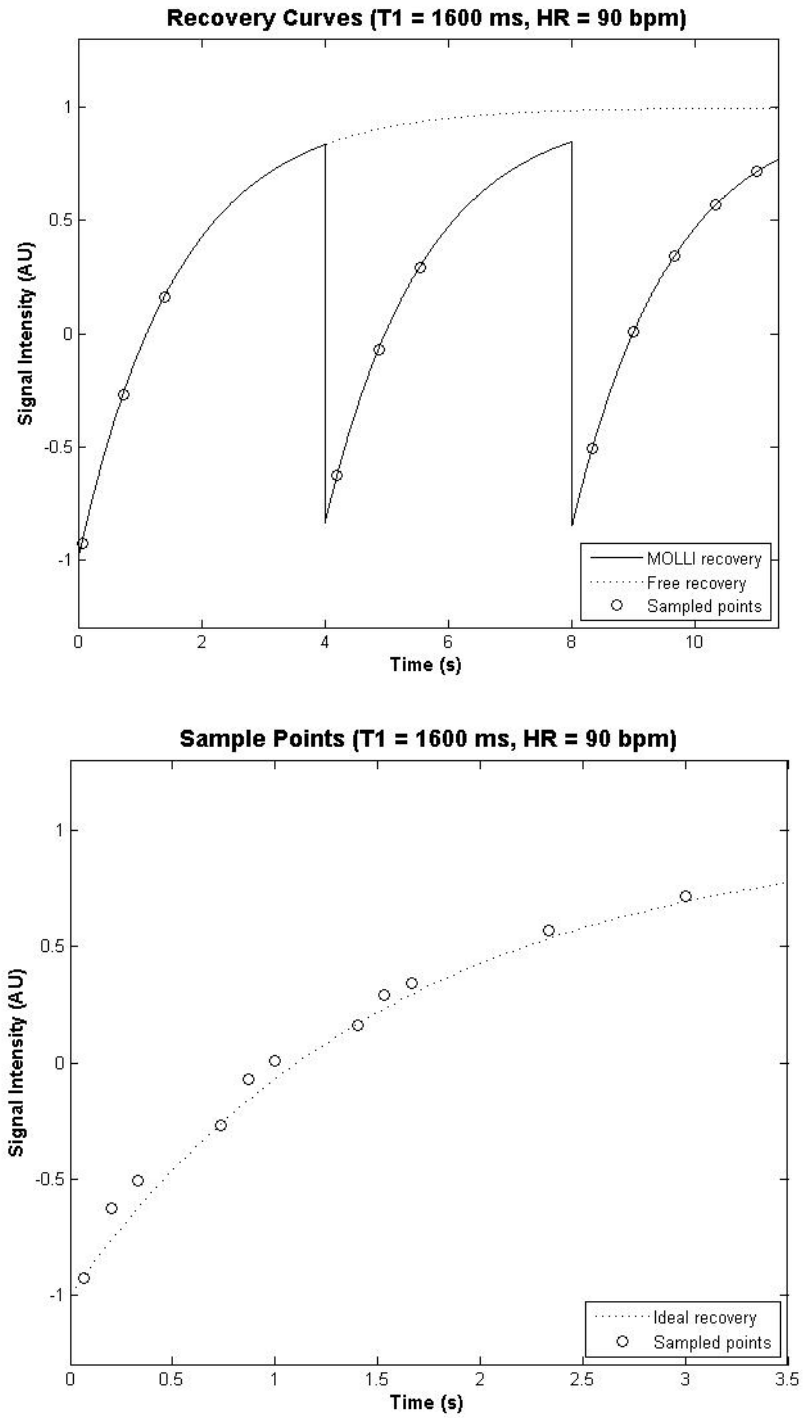

Figure 9. (top) Simulated recovery curves for the original MOLLI sequence (solid line, plus sample points) and free recovery (dashed line) for T_1 = 1600 ms, HR = 90 bpm. Magnetization does not recover completely prior to the second and third inversion pulses for the original MOLLI sequence. **(bottom)** Sample points from simulated recovery curve for the original MOLLI sequence, plotted with ideal recovery curve (T_1 = 1600 ms, HR = 90 bpm). All sample points acquired following the second and third inversion pulses reside above the ideal recovery curve. A fit to the entire group of sample points will result in an estimated T_1 of less than the ideal value.

In conclusion, this study has demonstrated measurement of normal and hyperoxic myocardial and LV blood T_1 values at 3.0 T with the single breath-hold MOLLI technique. There was a small reduction in mean myocardial T_1 during inhalation of pure oxygen at 3.0 T. However, the effectiveness of oxygen as a contrast agent in myocardial tissue was reduced compared to lower field strengths. Alternative T_1 measurement sequences based on the MOLLI technique have been presented and shown to be more accurate and consistent than the original MOLLI technique for relevant T_1 values at 3.0 T. Reliable T_1 measurements for pre and post-contrast myocardium can be achieved at 3.0 T with the use of a single inversion technique such as the presented MOLLI Alt 17-1 sequence.

CHAPTER III

THEORETICAL EFFECT OF HYPEROXIA ON MYOCARDIAL T_1

Introduction

A two-compartment, fast-exchange model has been proposed by Bauer et al (31) to calculate the theoretical effect of an intravascular contrast agent (IVCA) on myocardial T_1. T_1 relaxation in the myocardium is modeled as a function of regional blood volume (RBV) and perfusion (P) with the assumption that measured magnetization recovery is influenced only by the longitudinal relaxation rates of spins located in the intracapillary and extravascular spaces, neglecting the contribution from larger blood vessels. The exchange rate of magnetic spins between these two compartments is considered to be much greater than the relaxation rate within either compartment (17).

In the two-compartment, fast-exchange model, the presence of an IVCA causes the relaxation time of the arterial blood supplying the capillaries to decrease relative to the pre-contrast state, while the relaxation time of the extravascular tissue remains constant. This assumption is applied to oxygen as a contrast agent in this study even though oxygen is capable of freely diffusing into the extravascular tissue. In this application of the model, the concentration of oxygen within the extravascular space is assumed to not change significantly with hyperoxia. If the concentration of oxygen in the extravascular

tissue remains relatively constant, the relaxation time of the tissue independent of the blood would also not change significantly.

This assumption regarding the hyperoxic concentration of oxygen within the extravascular space bears scrutiny as it is fundamental to the application of the two-compartment model to oxygen as a contrast agent. Although the concentration of molecular oxygen in the blood increases during inhalation of pure oxygen (23), hyperoxia is known to induce vasoconstriction and subsequent reduction in capillary density in tissues throughout the body, including the myocardium (32,33). These hyperoxic responses decrease the amount of blood available for oxygen exchange with extravascular tissue. In addition, an increase in myoglobin saturation levels in the myocardium will at least partially mitigate an increase in molecular oxygen concentration (34). The net result of these effects on the concentration of molecular oxygen within the tissues has not been quantified.

The role of hyperoxia on oxygen delivery and consumption has been investigated and can perhaps provide some insight into the tissue concentration of oxygen (35). Prior studies have shown that neither total oxygen consumption nor delivery increase in humans with hyperoxia (36,37). The increase in molecular oxygen in the blood does not lead to an increase in the rate of cellular respiration or oxygen uptake in the tissues at equilibrium. There is some evidence of a wash-in effect in the first minutes of pure oxygen inhalation, which could potentially contribute to an increase in the extravascular concentration of molecular oxygen (37). However, this potential increase has not been demonstrated or

quantified. For the purposes of this application of the two-compartment, fast-exchange model, it is assumed that there is no increase in the concentration of molecular oxygen in the extravascular space of the myocardium.

This chapter documents the major equations and assumptions used in the model for this research. The estimated hyperoxic T_1 of myocardium derived from the model is reported and compared to experimental results from Chapter 2.

Materials and Methods

Effective myocardial relaxation time ($T_{1,m}$), incorporating the relaxation of both intracapillary space and extravascular tissue, is defined as

$$T_{1,m} = \frac{1}{\lambda}\left(1 + P \cdot T_{1,a}\right), \quad [3]$$

where $T_{1,a}$ is the relaxation time of the arterial blood supplied to the capillaries (31). The variable λ represents the RBV and perfusion (P) weighted relaxation rate of the spins exchanged between the two compartments and is defined by

$$\lambda = \left(RBV \cdot T_{1,a}^{-1} + \left(1 - RBV\right) \cdot T_{1,evt}^{-1}\right) + P\,, \qquad [4]$$

where $T_{1,evt}$ is the relaxation time of spins in the extravascular tissue space and is independent of the relaxation rate of the blood (31). RBV was assumed to include only the intracapillary blood since almost all of the blood in the myocardium is contained

within the microcirculatory vessels (38). In addition, arterial and venous blood do not participate in spin exchange with the extravascular tissue and thus should not be included in the calculation of λ. RBV was valued at 0.04 $ml \cdot g^{-1}$ (31). P was assumed to be 0.93 $ml \cdot g^{-1} \cdot min^{-1}$ (39). Both RBV and P were assumed to decrease by 20% with hyperoxia (33).

$T_{1,evt}$ was calculated by first solving Eq. [3] for λ using the measured values of $T_{1,a}$ and $T_{1,m}$ under normal oxygenation ($T_{1,a}$(norm), $T_{1,m}$(norm), respectively) from the present study. Equation [4] was then solved for $T_{1,evt}$ using this calculated λ and measured $T_{1,a}$(norm).

Finally, theoretical $T_{1,m}$ during hyperoxia ($T_{1,m}$(oxy)) was determined using the calculated $T_{1,evt}$ and measured $T_{1,a}$(oxy) from the present study. Thus, the theoretical $T_{1,m}$(oxy) depends on the experimental $T_{1,a}$(oxy) and theoretical $T_{1,evt}$, which is calculated from experimental $T_{1,a}$(norm) and $T_{1,m}$(norm). Theoretical $T_{1,m}$(oxy) was then compared to the experimental $T_{1,m}$ (oxy) found in the in vivo study of the current work.

Results

Theoretical mean myocardial T_1 during hyperoxia ($T_{1,m}$(oxy)) was calculated using Eq. [3] as 1166 ms. This result matches very closely the experimental mean T_1 of myocardium during hyperoxia of 1165 ms and represents a predicted 0.8% decrease from the measured normal oxygenation value of 1175 ms. The RBV and perfusion weighted relaxation rate (λ) under hyperoxia was calculated with Eq. [4] as 0.872 $ml \cdot g^{-1} \cdot s^{-1}$. The

calculated value for $T_{1,evt}$ was 1159 ms. This value represents the theoretical longitudinal relaxation time of the extravascular cardiac tissue, excluding the blood within the tissue.

Discussion

Theoretical reduction in mean myocardial T_1 during hyperoxia as calculated with the two-compartment, fast-exchange model was 0.8%, which closely matched the measured reduction of 0.9%. This similarity provides further validation of the measured reduction in mean myocardial T_1 with hyperoxia in this study. The longitudinal relaxation time of cardiac extravascular tissue, independent of the blood contained within the volume of tissue, was calculated as 1159 ms. This value is only slightly less than the measured mean myocardial T_1 under normal oxygenation (1175 ms), which combines contributions from both extravascular tissue and blood. The small difference between these two values demonstrates the limited effect of intravascular T_1 on the measured longitudinal relaxation of cardiac tissue. This is consistent with published results indicating that intravascular contrast agents have a significantly smaller effect on myocardial T_1 than do extracellular contrast agents (40).

It is important to note that the theoretical reduction in myocardial T_1 with hyperoxia is highly dependent on the assumed values used for regional blood volume (RBV) and perfusion (P). There is a wide range of reported RBV's in the myocardium for humans, ranging from 4 – 13% (31,41,42,43). The larger values in this range estimate the total blood volume fraction, including all vessels, in a region of cardiac tissue. RBV in this study was chosen to be on the lower end of this range to represent only the intracapillary

blood that is able to exchange spins with the extravascular tissue. This value is consistent with capillary volume fraction found in small animals in prior studies (38). Arterial blood does not participate in spin-exchange in the two-compartment model and thus contributes to changes in T_1 only through a partial volume effect. This volume has been shown to be minimal in the myocardium of small animals (< 2%) and is not included in the theoretical model (44). Inhalation of pure oxygen does not affect the T_1 of venous blood (15,17). Thus, the fraction of RBV that contains post-capillary blood also should not be included in the calculation for the theoretical effect of hyperoxia on myocardial T_1. The value assumed for P (0.93 $ml \cdot g^{-1} \cdot min^{-1}$) for human myocardium was selected from a study that used a large number of patients across multiple research sites and is consistent with a large number of other published studies (39).

In conclusion, a theoretical model of the effect of hyperoxia on myocardial T_1 has been applied to validate the experimental results of Chapter 2. The assumptions necessary in order to apply this IVCA model to the use of oxygen as a contrast agent have been documented and examined. In this particular study, there is a high level of agreement between the predicted and measured reductions in mean myocardial T_1 during hyperoxia.

CHAPTER IV

CONCLUSIONS AND FUTURE WORK

Conclusions

This study has demonstrated measurement of normal and hyperoxic myocardial and LV blood T_1 values at 3.0 T with the single breath-hold MOLLI technique. There was a small reduction in mean myocardial T_1 during inhalation of pure oxygen at 3.0 T. However, the effectiveness of oxygen as a contrast agent in myocardial tissue was reduced compared to lower field strengths. A theoretical model of the effect of hyperoxia on myocardial T_1 has been applied to validate the experimental results. Alternative T_1 measurement sequences based on the MOLLI technique have been presented and shown to be more accurate and consistent than the original MOLLI technique. Reliable T_1 measurements for pre and post-contrast myocardium can be achieved at 3.0 T with the use of a single inversion technique such as the presented MOLLI Alt 17-1 sequence.

Future Work

Future research building on these results will investigate the apparent reduction in oxygen's effectiveness as a myocardial contrast agent at higher field strengths. The small sample size of experiments and the small number of subjects within each experiment quantifying the effect of inhalation of pure oxygen on myocardial T_1 make it difficult to definitively state the existence of this reduction in effectiveness. Measurement of

changes in T_1 with hyperoxia at 3.0 T can also be made on other tissues in the body, allowing for comparison with other published studies at lower field strengths.

In vivo measurements of both pre and post-contrast myocardial and LV blood T_1 should also be performed using the MOLLI Alt. 17-1 sequence. These T_1 values can be compared to the results of the current study as well as other published T_1 values for the myocardium and arterial blood at 3.0 T. A repeatability study tracking the same set of volunteers across a period of time could assess the consistency of this proposed sequence.

APPENDIX

Appendix A: Individual Subject Data

Experimental T_1 data for myocardium and LV blood pool of all subjects in the study.

Subject	Age	M/F	Normal Myocardium				Hyperoxic Myocardium				Normal LV Blood				Hyperoxic LV Blood			
			Mean HR (bpm)	Mean T1 (s)	Std Dev T1 (s)	Fit Coeff	Mean HR (bpm)	Mean T1 (s)	Std Dev T1 (s)	Fit Coeff	Mean T1 (s)	Std Dev T1 (s)	Fit Coeff		Mean T1 (s)	Std Dev T1 (s)	Fit Coeff	
224	24	F	78.9	1.130	0.076	0.988	75.0	1.100	0.064	0.995	1.321	0.075	0.983		1.200	0.066	0.991	
240	24	M	70.5	1.177	0.060	0.997	63.1	1.178	0.058	0.996	1.420	0.062	0.993		1.218	0.050	0.994	
264	22	M	64.8	1.157	0.055	0.994	63.2	1.134	0.065	0.997	1.583	0.054	0.995		1.500	0.051	0.996	
273	25	M	61.6	1.228	0.063	0.999	60.5	1.207	0.054	0.996	1.487	0.130	0.994		1.341	0.088	0.994	
282	25	F	60.0	1.188	0.115	0.996	55.4	1.179	0.079	0.995	1.509	0.072	0.995		1.367	0.084	0.994	
319	24	M	57.9	1.162	0.063	0.994	55.9	1.159	0.063	0.994	1.568	0.075	0.993		1.395	0.062	0.993	
328	26	M	64.2	1.217	0.056	0.997	62.9	1.200	0.059	0.997	1.539	0.071	0.995		1.358	0.073	0.996	
346	29	M	72.7	1.151	0.069	0.993	74.5	1.138	0.061	0.993	1.441	0.091	0.990		1.226	0.089	0.990	
380	32	M	63.2	1.181	0.078	0.993	49.6	1.202	0.098	0.992	1.491	0.088	0.990		1.435	0.081	0.992	
425	31	M	49.3	1.157	0.082	0.995	45.9	1.155	0.062	0.996	1.615	0.092	0.993		1.449	0.079	0.992	
Mean	26.2		64.3	1.175	0.072	0.995	60.6	1.165	0.066	0.995	1.497	0.081	0.992		1.349	0.072	0.993	
Std Dev	3.3		8.3	0.030			9.5	0.035			0.087				0.104			

Appendix B: Study Comparison Data

Data table for the calculation of the compartmental influence of oxygen as a contrast agent in the myocardium compared to arterial blood, characterized by the ratio of the change in relaxation rates for the two compartments with hyperoxia, $\Delta R_{1,myo} / \Delta R_{1,blood}$.

	Study						
	1.5T	2.0T	3.0T	1.5T study by Tadamura et al, 1997			
Myocardial T1				2.0T study by Fidler et al, 2004			
Normoxic (ms)	995	1389	1175				
Hyperoxic (ms)	966	1351	1165				
ΔT_{1myo} (ms)	-29	-38	-10				
ΔT_{1myo} (%)	-2.9%	-2.7%	-0.9%				
LV Blood T1							
Normoxic (ms)	1262	1709	1497				
Hyperoxic (ms)	1120	1423	1349				
ΔT_{1blood} (ms)	-142	-286	-148				
ΔT_{1blood} (%)	-11.3%	-16.7%	-9.9%				
ΔT1myo/ΔT1blood (ms/ms)	0.20	0.13	0.07				
ΔT1myo/ΔT1blood (%/%)	0.26	0.16	0.09				
Myocardial R1							
Normoxic (s^{-1})	1.005	0.720	0.851				
Hyperoxic (s^{-1})	1.035	0.740	0.858				
ΔR_{1myo} (s^{-1})	0.030	0.020	0.007				
ΔR_{1myo} (%)	3.0%	2.8%	0.9%				
LV Blood T1							
Normoxic (s^{-1})	0.792	0.585	0.668				
Hyperoxic (s^{-1})	0.893	0.703	0.741				
ΔR_{1blood} (s^{-1})	0.100	0.118	0.073				
ΔR_{1blood} (%)	12.7%	20.1%	11.0%				
ΔR1myo/ΔR1blood (s^{-1}/s^{-1})	0.30	0.17	0.10				
ΔR1myo/ΔR1blood (%/%)	0.24	0.14	0.08				

Appendix C: Matlab Code

The following section of code, named 'MOLLI_T1_calc_pixel_by_pixel.m', will report the mean and standard deviation of the T_1 values for all the pixels within a user-selected region of interest. It will also report the correlation coefficient for the sampled points vs. the ideal recovery curve characterized by the mean T_1.

```
%
% MOLLI_T1_calc_pixel_by_pixel.m
%
% Paul Hilt - July 2008
%
% This is based on Michael Nichols code for calculating T1 for an
% ROI in the lungs.
%
% It was modified by Paul Hilt for calculating T1 for all pixels in
% an ROI on a series of MOLLI images.  It will find the mean
% and standard deviation of the T1's for all the pixels in ROI.  It
% will also report the fit coefficient for the calculated T1 recovery
% curve vs. the sample points.
%
% This method calculates T1 using a three parameter fit model
% (A - B*exp(-t/T1*)) proposed by Deichmann & Haase.  It will report
% both T1* and corrected T1 values based on D & H:  T1 = T1* * (B/A -
1)
%
% This function can be executed stand-alone by modifying the
appropriate
% input parameters at the beginning of the file.
%

close all;
clear all;

%%%%%%%%%%%%%%%%%%%%%%%%%%%%%%%%%%%%%%%%%%%%%%%%%%%%%%%%%%%%%%%%%%%
% Input and Output file naming
%%%%%%%%%%%%%%%%%%%%%%%%%%%%%%%%%%%%%%%%%%%%%%%%%%%%%%%%%%%%%%%%%%%
data_dir = '..\MOLLI Data\346\';        % PAR/REC files directory
file = [data_dir,'CBP_346_20_1.PAR'];   % PAR file name
scan_num = 'Scan20';                    % Tag for naming output files
scan_tag = 'Scan20';                    % Tag for naming output dir
scan_label = '17RR - myocardium, oxygen';   % used to title figures &
plots
%%%%%%%%%%%%%%%%%%%%%%%%%%%%%%%%%%%%%%%%%%%%%%%%%%%%%%%%%%%%%%%%%%%
% END Input and Output file naming
%%%%%%%%%%%%%%%%%%%%%%%%%%%%%%%%%%%%%%%%%%%%%%%%%%%%%%%%%%%%%%%%%%%

scan_dir = [data_dir,scan_tag];         % Output directory name
```

```
output_dir = [scan_dir,'\'];
mkdir(scan_dir);

%%%%%%%%%%%%%%%%%%%%%%%%%%%%%%%%%%%%%%%%%%%%%%%%%%%%%%%%%%%%%%%%%%%%%%%
% Parameter Setup
%%%%%%%%%%%%%%%%%%%%%%%%%%%%%%%%%%%%%%%%%%%%%%%%%%%%%%%%%%%%%%%%%%%%%%%
% ROI setup
use_saved_roi = 0;                      % 0 = no, 1 = yes
use_saved_bkgd = 1;                     % 0 = no, 1 = yes
roi_label = 'myocard';                  % name of saved ROI
roi_file = [output_dir,roi_label];
roi_file_bkgd = [scan_dir,'\','bckgnd'];% name of background for SNR
calc
% usage of complex images
use_complex_images = 0;                 % 0 = no, 1 = yes
% Initial steady state cycle?
steady_state_cycle = 0;                 % 0 = no, 1 = yes
% Adjust # of data points to flip
%
#########################################################################
% NOTE:  Optimal # of flip points must be determined manually by
adjusting
% this value and determining highest fit coefficient for corresponding
T1.
%
#########################################################################
flip_points = 3;
% Select image number for selection of ROIs
roi_image_num = 1;                      % image number from original
order

% The MOLLI code uses (up to) three imaging trains, each with
% a different inversion time.  Here we set up which cycles
% contain the inversion pulse, what the inversion time is for
% each pulse and how many images make up each train.
% Note for one or two cycle trains, set 'train[2|3]_dur = 0'

train1_beg = 1;     % cycle number of first inversion pulse
train1_dur = 3;     % number of imaging cycles in first train
train1_inv = 0.1;   % inversion time for first train

train2_beg = 7;
train2_dur = 3;
train2_inv = 0.3;

train3_beg = 13;
train3_dur = 5;
train3_inv = 0.5;

%%%%%%%%%%%%%%%%%%%%%%%%%%%%%%%%%%%%%%%%%%%%%%%%%%%%%%%%%%%%%%%%%%%%%%%
% END Parameter Setup
%%%%%%%%%%%%%%%%%%%%%%%%%%%%%%%%%%%%%%%%%%%%%%%%%%%%%%%%%%%%%%%%%%%%%%%

% Read PAR/REC files
[dataT1,parmsT1,dimsT1]=ReadParRec(file);
```

```
[row, col, rr_cycles] = size(dataT1);

%%%%%%%%%%%%%%%%%%%%%%%%%%%%%%%%%%%%%%%%%%%%%%%%%%%%%%%%%%%%%%%%%%%%%%%
% ROI selection
%%%%%%%%%%%%%%%%%%%%%%%%%%%%%%%%%%%%%%%%%%%%%%%%%%%%%%%%%%%%%%%%%%%%%%%

if (use_saved_roi == 0)
    figure
    imagesc(dataT1(:,:,roi_image_num));
    colormap(gray);
    title('Select ROI by clicking on vertices of a polygon');
    [mask_m, X_v, Y_v] = roipoly;
    save(roi_file, 'mask_m', 'X_v', 'Y_v');
else
    load(roi_file);
end

%if ((use_saved_bkgd == 0)&&(use_saved_roi == 0))
if (use_saved_bkgd == 0)
    figure
    imagesc(dataT1(:,:,rr_cycles));
    title('Select ROI of background region for noise calculation');
    [bgnd_m, nX_v, nY_v] = roipoly;
    save(roi_file_bkgd, 'bgnd_m', 'nX_v', 'nY_v');
else
    load(roi_file_bkgd);
    figure
    imagesc(dataT1(:,:,rr_cycles));
    line(nX_v,nY_v);
end

%%%%%%%%%%%%%%%%%%%%%%%%%%%%%%%%%%%%%%%%%%%%%%%%%%%%%%%%%%%%%%%%%%%%%%%
% Magnitude image section:
%%%%%%%%%%%%%%%%%%%%%%%%%%%%%%%%%%%%%%%%%%%%%%%%%%%%%%%%%%%%%%%%%%%%%%%

% Find magnitude images from dynamic images using image_type_mr
% (field 5 in v4 ParRec) if complex images are used.
% NOTE:  not sure this works... (pjh)
if (use_complex_images == 1)
    for i=1:rr_cycles
        % find magnitude images
        %if (parmsT1.tags(i,5) == 0)
        %Try this with magnitude & phase images:  (01/28/08)
        if (mod(parmsT1.tags(i,7),2) == 0)
            % assign dyn_scan_begin_time for magnitude image specified
by
            % the dynamic_scan_number value in tag 3
            dyn_scan_times_temp(parmsT1.tags(i,3)) =
parmsT1.tags(i,32);
            % assign image to temporary 3D matrix
            tempImg(:,:,parmsT1.tags(i,3)) = dataT1(:,:,i);
        end
    end
    % decrease image_count by one to get true number of images
    rr_cycles = parmsT1.tags(i,3);
    % clear dataT1 and reassign tempImg to dataT1
```

```
    clear dataT1;
    dataT1 = tempImg;
    dyn_scan_times = dyn_scan_times_temp(2:rr_cycles);
else
    % Set up dyn_scan_time array with dyn_scan_begin_time values
    % (field 32 in v4 ParRec)
    dyn_scan_times = parmsT1.tags(2:rr_cycles,32)';
end

% *******************************************************
% Must update dyn_scan_times(rr_cycles) with an estimated value
% using the previous two values b/c ParRec file does not contain
% this value for the final dynamic image acquired.
% In this case, the time between images n-2 and n-1 is duplicated
% for the elapsed time between image n-1 and n.
% *******************************************************
dyn_scan_times(rr_cycles) =  (2 * dyn_scan_times(rr_cycles-1)) -
dyn_scan_times(rr_cycles-2);

%%%%%%%%%%%%%%%%%%%%%%%%%%%%%%%%%%%%%%%%%%%%%%%%%%%%%%%%%%%%%%%
% Reorder images based on effective TI
%%%%%%%%%%%%%%%%%%%%%%%%%%%%%%%%%%%%%%%%%%%%%%%%%%%%%%%%%%%%%%%

% number of cycles in scan sequences
scan_seq_cycles = rr_cycles;

% initialize n_images, which contains the number of images used
% to calculate T1 from the MOLLI sequence
n_images = 1;

% set inversion time for initial image
inv_time(n_images) = train1_inv;
% T1_image array contains only the images used to calculate T1.
% The non-imaging cycle data is eliminated.
T1_image(:,:,n_images) = dataT1(:,:,train1_beg);

for i=train1_beg+1:train1_beg + train1_dur - 1
    n_images = n_images + 1;
    inv_time(n_images) = train1_inv + dyn_scan_times(i) -
dyn_scan_times(train1_beg);
    T1_image(:,:,n_images) = dataT1(:,:,i);
end

if (train2_dur > 0)
    n_images = n_images + 1;
    inv_time(n_images) = train2_inv;
    T1_image(:,:,n_images) = dataT1(:,:,train2_beg);
end

for i=train2_beg+1:train2_beg + train2_dur - 1
    n_images = n_images + 1;
    inv_time(n_images) = train2_inv + dyn_scan_times(i) -
dyn_scan_times(train2_beg);
    T1_image(:,:,n_images) = dataT1(:,:,i);
end
```

```
if (train3_dur > 0)
    n_images = n_images + 1;
    inv_time(n_images) = train3_inv;
    T1_image(:,:,n_images) = dataT1(:,:,train3_beg);
end

for i=train3_beg+1:train3_beg + train3_dur - 1
    n_images = n_images + 1;
    inv_time(n_images) = train3_inv + dyn_scan_times(i) -
dyn_scan_times(train3_beg);
    T1_image(:,:,n_images) = dataT1(:,:,i);
end

% if a steady state cycle exists (steady_state_cycle = 1), set
% inv_time for first image to something large.
for i=1:steady_state_cycle
    n_images = n_images + 1;
    inv_time(n_images) = 20;
    T1_image(:,:,n_images) = dataT1(:,:,i);
end

%%%%%%%%%%%%%%%%%%%%%%%%%%%%%%%%%%%%%%%%%%%%%%%%%%%%%%%%%%%%%%%%%%%%%%%
% Sort images by inversion time
%%%%%%%%%%%%%%%%%%%%%%%%%%%%%%%%%%%%%%%%%%%%%%%%%%%%%%%%%%%%%%%%%%%%%%%
[sTimes,sIndex] = sort(inv_time);
clear Times;        % inversion times for each images
clear dataT1;       % image data, in order by ascending TI
count = 1;
for i=1:n_images
    dataT1(:,:,count) = T1_image(:,:,sIndex(i));
    Times(count) = sTimes(i);
    count = count + 1;
end

%%%%%%%%%%%%%%%%%%%%%%%%%%%%%%%%%%%%%%%%%%%%%%%%%%%%%%%%%%%%%%%%%%%%%%%
% Image display
%%%%%%%%%%%%%%%%%%%%%%%%%%%%%%%%%%%%%%%%%%%%%%%%%%%%%%%%%%%%%%%%%%%%%%%

% parameters for composite image display
clims = [0 max(max(max(dataT1)))];
num_images_div_2 = ceil(n_images/2);
composite_image = zeros(2*row,num_images_div_2*col);

figure;
for n=1:n_images
    subplot(5,4,n)
    imagesc(dataT1(:,:,n));
    colormap(gray);
    title_string = ['Image ',num2str(n), ' - ',scan_label];
    title(title_string);
    figure;
    %create a single image with no spaces
    if (n <= num_images_div_2)
        r_start = 1;
```

```
        r_end = row;
        c_start = (n - 1)* col + 1;
        c_end = n * col;
    else
        r_start = row + 1;
        r_end = 2 * row;
        c_start = (n - num_images_div_2 - 1) * col + 1;
        c_end = (n - num_images_div_2) * col;
    end
    composite_image(r_start:r_end,c_start:c_end) = dataT1(:,:,n);
    imagesc(dataT1(:,:,n));
    hold on;
    colormap(gray);
    colorbar;
    line(X_v,Y_v);
    title_string2 = ['TI = ',num2str(Times(n),'%10.3f'), ' -
',scan_label];
    title(title_string2);
    output_file =
[output_dir,roi_label,'_','Image',num2str(n),scan_num,'.jpg'];
    saveas(gcf,output_file);
    close;
end
output_file = [output_dir,'DecaySeq',scan_num,'.jpg'];
saveas(gcf,output_file);
figure;
imagesc(composite_image);
colormap(gray);
axis off;
output_file = [output_dir,'CompSeq',scan_num,'.jpg'];
saveas(gcf,output_file);

%%%%%%%%%%%%%%%%%%%%%%%%%%%%%%%%%%%%%%%%%%%%%%%%%%%%%%%%%%%%%%%%%%%%
% ROI T1 Calculation
%%%%%%%%%%%%%%%%%%%%%%%%%%%%%%%%%%%%%%%%%%%%%%%%%%%%%%%%%%%%%%%%%%%%

%initialize A, B, T1_star and T1 vectors
A = zeros(row,col);
B = zeros(row,col);
T1 = zeros(row,col);
T1_star = zeros(row,col);
CC_star_m = zeros(row,col);
CC_m = zeros(row,col);
SI = zeros(row,col,length(Times));
M0 = zeros(row,col);


for i=1:row
    for j=1:col
        if (mask_m(i,j) ~= 0)
            SigInt = squeeze(dataT1(i,j,:))';
            % flip polarity (to negative) of first 'flip_points'
samples
            for n = 1:flip_points
                SigInt(n) = - SigInt(n);
            end
```

```
            % Fit using three parameter model
            [estimates, model] = fitcurvedemo3(Times,SigInt);
            A(i,j) = estimates(1);
            B(i,j) = estimates(2);
            R1_star = estimates(3);
            T1_star(i,j) = 1/R1_star;
            SI(i,j,:) = SigInt;

            % Find corrected T1 by Deichmann & Haase method (see above)
            T1(i,j) = T1_star(i,j) * (B(i,j) / A(i,j) - 1);
            M0(i,j) = A(i,j) * T1(i,j) / T1_star(i,j);
            CC_star_temp = corrcoef(Est_star,SigInt);
            CC_star_m(i,j) = CC_star_temp(2,1);
            CC_temp = corrcoef(Est,SigInt);
            CC_m(i,j) = CC_temp(2,1);

        else
            %redundant
            A(i,j) = 0;
            B(i,j) = 0;
            T1_star(i,j) = 0;
            T1(i,j) = 0;
            CC_star_m(i,j) = 0;
            CC_m(i,j) = 0;
            M0(i,j) = 0;
        end
    end
end

%%%%%%%%%%%%%%%%%%%%%%%%%%%%%%%%%%%%%%%%%%%%%%%%%%%%%%%%%%%%%%%%%%%%%%%
% SNR calculation section
%%%%%%%%%%%%%%%%%%%%%%%%%%%%%%%%%%%%%%%%%%%%%%%%%%%%%%%%%%%%%%%%%%%%%%%

% NOTE:  Not sure how valid this is, use only for relative comparisons
% (pjh)

%find estimate of SNR using mean & std dev of signal intensity in ROI
for i=1:n_images
    masked_sig = mask_m .* dataT1(:,:,i);
    noise_v(i) = std2(masked_sig(masked_sig>0));
    sig_v(i) = mean(mean(masked_sig(masked_sig>0)));
end
snr_roi = sig_v(n_images)/noise_v(n_images);

%find estimate of SNR using mean signal intensities in ROI & background
masked_bgnd = bgnd_m .* dataT1(:,:,n_images);
noise_bgnd = std2(masked_bgnd(masked_bgnd>0));

%test whether there are at least 500 non-zero pixels in noise region
if (sum(sum(masked_bgnd>0)) > 500)
    snr_img = sig_v(n_images)/noise_bgnd;
else
    snr_img = NaN;
end
```

```
%number of pixels in ROI
Denom_v = sum(sum(mask_m));

%%%%%%%%%%%%%%%%%%%%%%%%%%%%%%%%%%%%%%%%%%%%%%%%%%%%%%%%%%%%%%%%%%%%%%%
% Output section
%%%%%%%%%%%%%%%%%%%%%%%%%%%%%%%%%%%%%%%%%%%%%%%%%%%%%%%%%%%%%%%%%%%%%%%

%Estimates for signal intensities at each time in vector Times
%based on the determined parameters for A,B & T1*
Est = zeros(length(Times));
Est_star = zeros(length(Times));

%Estimates at each time in vector TimeInt, a more tightly spaced
%time interval for plotting curves based on calculated T1.
TimeInt = 0:0.05:max(Times);
PlotEst = zeros(length(TimeInt));
PlotEst_star = zeros(length(TimeInt));

%calculate average and standard deviations of T1 & T1*
T1_ave = mean(T1(T1>0));
T1_std = std(T1(T1>0));
T1_star_ave = mean(T1_star(T1_star>0));
T1_star_std = std(T1_star(T1_star>0));
A_ave = mean(A(A>0));
B_ave = mean(B(B>0));
CC_star_ave = mean(CC_star_m(CC_star_m~=0));
CC_ave = mean(CC_m(CC_m~=0));
M0_ave = mean(M0(M0~=0));

%find average signal intensity within ROI for each image
for i=1:length(Times)
    SI_temp = SI(:,:,i);
    SI_ave(i) = mean(SI_temp(SI_temp~=0));
end

%calculate signal intensity values based on determined parameters
%A,B & T1* at sample points (Est_star) and for plot (PlotEst_star),
%also calculate correlation coefficient to averaged SI values
%at each time point
Est_star = A_ave - (B_ave .* exp(-Times/T1_star_ave));
CC_star = corrcoef(Est_star,SI_ave);
PlotEst_star = A_ave - (B_ave .* exp(-TimeInt/T1_star_ave));
%same as above for T1
Est = M0_ave * (1 - (2 .* exp(-Times/T1_ave)));
PlotEst = M0_ave * (1 - (2 .* exp(-TimeInt/T1_ave)));
CC = corrcoef(Est,SI_ave);

%create plot for sample points & T1* curve
figure
h = axes('Position',[0 0 1 1],'Visible','off');
axes('Position',[.1 .1 .82 .72]);
plot(Times, SI_ave, 'bo', TimeInt, PlotEst_star(1,:), 'g-')
title_string = ['T1 star (pixel ave.) - ',scan_label];
title(title_string);
```

```
xlabel('time (ms)');
ylabel('intensity (AU)');
set(gcf,'CurrentAxes',h)
text(0.78,0.97,['T1* = ',num2str(T1_star_ave,'%5.3f'),' +/-
',num2str(T1_star_std,'%5.3f')]);
text(0.78,0.94,['r   = ',num2str(CC_star_ave,'%5.3f')]);
text(0.78,0.91,['SNR = ',num2str(snr_img,'%5.2f')]);
text(0.78,0.88,['sig/sd(roi) = ',num2str(snr_roi,'%5.2f')]);output_file
= [output_dir,'T1star_',roi_label,scan_num,'.jpg'];
text(0.78,0.85,['noise sig = ',num2str(noise_bgnd,'%4.1f')]);
saveas(gcf,output_file);

%create plot for sample points and T1 curve
figure
h = axes('Position',[0 0 1 1],'Visible','off');
axes('Position',[.1 .1 .82 .72]);
plot(Times, SI_ave, 'bo', TimeInt, PlotEst, 'g-')
title_string = ['T1 corr. (pixel ave.) - ',scan_label];
title(title_string);
xlabel('time (ms)');
ylabel('intensity (AU)');
set(gcf,'CurrentAxes',h)
text(0.78,0.97,['T1 = ',num2str(T1_ave,'%5.3f'),' +/-
',num2str(T1_std,'%5.3f')]);
text(0.78,0.94,['r  = ',num2str(CC_ave,'%5.3f')]);
text(0.78,0.91,['SNR = ',num2str(snr_img,'%5.2f')]);
text(0.78,0.88,['sig/sd(roi) = ',num2str(snr_roi,'%5.2f')]);
text(0.78,0.85,['noise sig = ',num2str(noise_bgnd,'%4.1f')]);
output_file = [output_dir,'T1corr_',roi_label,scan_num,'.jpg'];
saveas(gcf,output_file);
```

Functions used in 'MOLLI_T1_calc_pixel_by_pixel.m':

'readParRec.m' – standard parser for header data in .PAR files

'fitcurvedemo3.m':

```
function [estimates, model] = fitcurvedemo3(Times, Mag6)
% Call fminsearch with a random starting point.
start_point = [250000 500000 1]; %was 4500
oldopts = optimset('fminsearch');
options = optimset(oldopts,'MaxFunEvals',5000);
model = @expfun;
estimates = fminsearch(model, start_point,options);
% expfun accepts curve parameters as inputs, and outputs sse,
% the sum of squares error for the sample points
% and the FittedCurve. FMINSEARCH only needs sse, but we want to
% plot the FittedCurve at the end.
    function [sse, FittedCurve] = expfun(params)
        A = params(1);
        B = params(2);
        R1_star = params(3);
        FittedCurve = A - (B .* exp(-1 * R1_star .* Times));
        ErrorVector = FittedCurve - Mag6;
```

```
            sse = sum(ErrorVector .^ 2);
        end
    end
```

REFERENCES

1. Rosamond W, Flegal K, Furie K, Go A, Greenlund K, Haase N, Hailpern SM, Ho M, Howard V, Kissela B, Kittner S, Lloyd-Jones D, McDermott M, Meigs J, Moy C, Nichol G, O'Donnell C, Roger V, Sorlie P, Steinberger J, Thom T, Wilson M, Hong Y. Heart disease and stroke statistics - 2008 update - A report from the American Heart Association Statistics Committee and Stroke Statistics Subcommittee. Circulation 2008;117(4):E25-E146.

2. Haacke EM. Magnetic Resonance Imaging: Physical Principles and Sequence Design. New York: Wiley; 1999. xxvii, 914 p.

3. Gutberlet M, Noeske R, Schwinge K, Freyhardt P, Felix R, Niendorf TF. Comprehensive cardiac magnetic resonance imaging at 3.0 tesla - Feasibility and implications for clinical applications. Invest Radiol 2006;41(2):154-167.

4. Sakuma H. Magnetic resonance imaging for ischemic heart disease. J Magn Reson Imaging 2007;26(1):3-13.

5. Finn JP, Nael K, Deshpande V, Ratib O, Laub G. Cardiac MR imaging: State of the technology. Radiology 2006;241(2):338-354.

6. Messroghli DR, Walters K, Plein S, Sparrow P, Friedrich MG, Ridgway JP, Sivananthan MU. Myocardial T1 mapping: Application to patients with acute and chronic myocardial infarction. Magn Reson Med 2007;58(1):34-40.

7. Alfidi RJ, Haaga JR, Elyousef SJ, Bryan PJ, Fletcher BD, Lipuma JP, Morrison SC, Kaufman B, Richey JB, Hinshaw WS, Kramer DM, Yeung HN, Cohen AM, Butler HE, Ament AE, Lieberman JM. Preliminary experimental results in humans and animals with a superconducting, whole-body, nuclear magnetic resonance scanner. Radiology 1982;143(1):175-181.

8. Doyle FH, Gore JC, Pennock JM. Relaxation rate enhancement observed in vivo by NMR imaging. J Comput Assist Tomogr 1981;5(2):295-296.

9. Tadamura E, Hatabu H, Li W, Prasad PV, Edelman RR. Effect of oxygen inhalation on relaxation times in various tissues. J Magn Reson Imaging 1997;7(1):220-225.

10. Fidler F, Wacker CM, Dueren C, Weigel M, Jakob PM, Bauer WR, Haase A. Myocardial perfusion measurements by spin-labeling under different vasodynamic states. J Cardiovasc Magn Reson 2004;6(2):509-516.

11. Messroghli DR, Radjenovic A, Kozerke S, Higgins DM, Sivananthan MU, Ridgway JP. Modified Look-Locker inversion recovery (MOLLI) for high-resolution T1 mapping of the heart. Magn Reson Med 2004;52(1):141-146.

12. Messroghli DR, Plein S, Higgins DM, Walters K, Jones TR, Ridgway JP, Sivananthan MU. Human myocardium: Single-breath-hold MR T1 mapping with high spatial resolution - Reproducibility study. Radiology 2006;238(3):1004-1012.

13. Bauner KU, Muehling O, Wintersperger BJ, Winnik E, Reiser MF, Huber A. Inversion recovery single-shot TurboFLASH for assessment of myocardial infarction at 3 Tesla. Invest Radiol 2007;42(6):361-371.

14. Bernstein MA, Huston J, Ward HA. Imaging artifacts at 3.0T. J Magn Reson Imaging 2006;24(4):735-746.

15. Schar M, Kozerke S, Fischer SE, Boesiger P. Cardiac SSFP imaging at 3 Tesla. Magn Reson Med 2004;51(4):799-806.

16. Detre JA, Leigh JS, Williams DS, Koretsky AP. Perfusion imaging. Magn Reson Med 1992;23(1):37-45.

17. Schwarzbauer C, Syha J, Haase A. Quantification of regional blood volumes by rapid T1 mapping. Magn Reson Med 1993;29(5):709-712.

18. Wacker CM, Fidler F, Dueren C, Hirn S, Jakob PM, Ertl G, Haase A, Bauer WR. Quantitative assessment of myocardial perfusion with a spin-labeling technique: Preliminary results in patients with coronary artery disease. J Magn Reson Imaging 2003;18(5):555-560.

19. Krombach GA, Hahn C, Tomars M, Buecker A, Grawe A, Gunther RW, Kuhl HP. Cardiac amyloidosis: MR imaging findings and T1 quantification, comparison with control subjects. J Magn Reson Imaging 2007;25(6):1283-1287.

20. Hosch W, Bock M, Libicher M, Ley S, Hegenbart U, Dengler TJ, Katus HA, Kauczor HU, Kauffmann GW, Kristen AV. MR-relaxometry of myocardial tissue - Significant elevation of T1 and T2 relaxation times in cardiac amyloidosis. Invest Radiol 2007;42(9):636-642.

21. Thomson AJ, Webb DJ, Maxwell SRJ, Grant IS. Oxygen therapy in acute medical care - The potential dangers of hyperoxia need to be recognised. BMJ 2002;324(7351):1406-1407.

22. West JB. Respiratory Physiology -- The Essentials. Baltimore: Williams & Wilkins; 1995. 193 p.

23. d'Othee BJ, Rachmuth G, Munasinghe J, Lang EV. The effect of hyperoxygenation on T1 relaxation time in vitro. Acad Radiol 2003;10(8):854-860.

24. Noseworthy MD, Kim JK, Stainsby JA, Stanisz GJ, Wright GA. Tracking oxygen effects on MR signal in blood and skeletal muscle during hyperoxia exposure. J Magn Reson Imaging 1999;9(6):814-820.

25. Wansapura J, Gottliebson W, Crotty E, Fleck R. Cyclic variation of T1 in the myocardium at 3 T. Magn Reson Imaging 2006;24(7):889-893.

26. Look DC, Locker DR. Time saving in measurement of NMR and EPR relaxation times. Rev Sci Instrum 1970;41(2):250-251.

27. Deichmann R, Haase A. Quantification of T1 values by Snapshot-FLASH NMR imaging. J Magn Reson 1992;96(3):608-612.

28. Nekolla S, Gneiting T, Syha J, Deichmann R, Haase A. T1 maps by k-space reduced Snapshot-FLASH MRI. J Comput Assist Tomogr 1992;16(2):327-332.

29. Sharma P, Socolow J, Patel S, Pettigrew RI, Oshinski JN. Effect of Gd-DTPA-BMA on blood and myocardial T1 at 1.5T and 3T in humans. J Magn Reson Imaging 2006;23(3):323-330.

30. Scheffler K, Hennig J. T1 quantification with inversion recovery TrueFISP. Magn Reson Med 2001;45(4):720-723.

31. Bauer WR, Hiller KH, Roder F, Rommel E, Ertl G, Haase A. Magnetization exchange in capillaries by microcirculation affects diffusion-controlled spin-relaxation: A model which describes the effect of perfusion on relaxation enhancement by intravascular contrast agents. Magn Reson Med 1996;35(1):43-55.

32. Bergofsky EH, Bertun P. Response of regional circulations to hyperoxia. J Appl Physiol 1966;21(2):567-572.

33. McNulty PH, Robertson BJ, Tulli MA, Hess J, Harach LA, Scott S, Sinoway LI. Effect of hyperoxia and vitamin C on coronary blood flow in patients with ischemic heart disease. J Appl Physiol 2007;102(5):2040-2045.

34. Ordway GA, Garry DJ. Myoglobin: an essential hemoprotein in striated muscle. J Exp Biol 2004;207(20):3441-3446.

35. Tsai AG, Cabrales P, Winslow RM, Intaglietta M. Microvascular oxygen distribution in awake hamster window chamber model during hyperoxia. Am J Physiol 2003;285(4):H1537-H1545.

36. Reinhart K, Bloos F, Konig F, Bredle D, Hannemann L. Reversible decrease of oxygen consumption by hyperoxia. Chest 1991;99(3):690-694.

37. Rousseau A, Bak Z, Janerot-Sjoberg B, Sjoberg F. Acute hyperoxaemia-induced effects on regional blood flow, oxygen consumption and central circulation in man. Acta Physiol Scand 2005;183(3):231-240.

38. Wei K, Kaul S. The coronary microcirculation in health and disease. Cardiol Clin 2004;22(2):221-231.

39. Iida H, Yokoyama I, Agostini D, Banno T, Kato T, Ito K, Kuwabara Y, Oda Y, Otake T, Tamura Y, Tadamura E, Yoshida T, Tamaki N. Quantitative assessment of regional myocardial blood flow using oxygen-15-labelled water and positron emission tomography: a multicentre evaluation in Japan. Eur J Nucl Med 2000;27(2):192-201.

40. Saeed M, Higgins CB, Geschwind JF, Wendland MF. T1-relaxation kinetics of extracellular, intracellular and intravascular MR contrast agents in normal and acutely reperfused infarcted myocardium using echo-planar MR imaging. Eur Radiol 2000;10(2):310-318.

41. Wilke N, Kroll K, Merkle H, Wang Y, Ishibashi Y, Xu Y, Zhang JN, Jeroschherold M, Muhler A, Stillman AE, Bassingthwaighte JB, Bache R, Ugurbil K. Regional myocardial blood volume and flow - First-pass MR imaging with polylysine-Gd-DTPA. J Magn Reson Imaging 1995;5(2):227-237.

42. Wacker CM, Wiesmann F, Bock M, Jakob P, Sandstede JJW, Lehning A, Ertl G, Schad LR, Haase A, Bauer WR. Determination of regional blood volume and intra-extracapillary water exchange in human myocardium using feruglose: First clinical results in patients with coronary artery disease. Magn Reson Med 2002;47(5):1013-1016.

43. Vogel R, Indermuhle A, Reinhardt J, Meier P, Siegrist PT, Namdar M, Kaufmann PA, Seiler C. The quantification of absolute myocardial perfusion in humans by contrast echocardiography - Algorithm and validation. J Am Coll Cardiol 2005;45(5):754-762.

44. Judd RM, Levy BI. Effects of barium-induced cardiac contraction on large-vessel and small-vessel intramyocardial blood volume. Circ Res 1991;68(1):217-225.